Humic surface waters of frozen peat bogs (permafrost zone) are highly resistant to bio- and photodegradation

Liudmila S. Shirokova[1,2], Artem V. Chupakov[2], Svetlana A. Zabelina[2], Natalia V. Neverova[2], Dahedrey Payandi-Rolland[1], Carole Causserand[1], Jan Karlsson[3], Oleg S. Pokrovsky[1,4]*

[1] Geoscience and Environment Toulouse, UMR 5563 CNRS, University of Toulouse, 14 Avenue Edouard Belin, Toulouse 31400, France
[2] Institute of Ecological Problems of the North, N. Laverov Federal Center for Integrated Arctic Research, Nab Severnoi Dviny 23, Arkhangelsk 163000, Russia
[3] Climate Impacts Research Centre (CIRC), Department of Ecology and Environmental Science, Umeå University, 901 87 Umeå, Sweden
[4] BIO-GEO-CLIM Laboratory, Tomsk State University, 35 Lenina Pr., Tomsk 634050, Russia

*corresponding author email: oleg.pokrovsky@get.omp.eu

Key words: depression, stream, river, organic carbon, photolysis, respiration, palsa, permafrost

Submitted to *Biogeosciences, after revision* May 2019

Abstract

Bio- and photo-degradation of dissolved organic matter (DOM) is identified as dominant vector of C cycle in boreal and high-latitude surface waters. In contrast to large number of studies of humic waters from permafrost-free regions and oligotrophic waters from permafrost-bearing regions, the bio- and photo-lability of DOM from humic surface waters of permafrost-bearing regions has not been thoroughly evaluated. Following standardized protocol, we measured biodegradation (low, intermediate, high temperature) and photodegradation (one intermediate temperature) of DOM in surface waters along the hydrological continuum (depression → stream → thermokarst lake → river Pechora) within a European Russian frozen peatland. In all systems, within the experimental resolution of 5 to 10%, there was no bio- or photodegradation of DOM over 1 month of incubation. It is possible that the main cause of the lack of degradation is the dominance of allochthonous refractory (soil, peat) DOM in all studied waters. Yet, all surface waters were supersaturated with CO_2. Thus, this study suggests that, rather than bio- and photo-degradation of DOM in the water column, other factors such as peat porewater DOM processing and respiration of sediments are the main drivers of elevated pCO_2 and emission in humic boreal waters of frozen peat bogs.

Introduction

Boreal and subarctic waters contain large amounts of plant, soil, and peat-originated dissolved organic matter (Wilkinson et al., 2013; Kaiser et al., 2017), and the proportion of land-derived organic carbon in waters is likely to increase with ongoing permafrost thaw (Wauthy et al., 2018). Heterotrophic bacteria degrade this DOM (Karlsson, 2007; McCallister and del Georgio, 2008), causing net heterotrophic conditions (Gross Primary Productivity < Respiration) and CO_2 emission to the atmosphere from surface waters (Ask et al., 2012; Lapierre et al., 2013). Between 10% and 40% of the dissolved organic carbon (DOC) in lakes, rivers and soil waters

of the boreal zone may be available for bacterial uptake over a time frame of several weeks (Berggren et al., 2010; Roehm et al., 2009). The biodegradability of DOM leached from permafrost and non-permafrost soils was recently reviewed by Vonk et al. (2015) who concluded that aquatic DOC is more biodegradable in regions with continuous permafrost compared to regions without permafrost. At the same time, among all Arctic rivers, the highest annual (20%) and winter (ca. 45%) biodegradable DOC (BDOC) was reported for the Ob River, draining through peatlands with minimal influence of permafrost (Wickland et al., 2012). Further, based on 14 studies of BDOC and their own research, Vonk et al. (2015) demonstrated zero BDOC loss in aquatic systems without permafrost, which is contradictory to general understanding of biodegradation of aquatic DOM as major driver of CO_2 emission in boreal waters. It is also important to note that all the available bio-degradation studies of inland waters in permafrost regions dealt with either tundra ecosystems with shallow peat soils overlaying the mineral substrate or mountain regions with essentially mineral soil substrates in Alaska or Canada (Holmes et al., 2008; Wickland et al., 2012; Ward et al., 2017) and with the yedoma soils of Eastern Siberia (Mann et al., 2014, 2015; Spencer et al., 2015).

Similarly, although the photolysis of DOM in boreal and subarctic aquatic environments contributes to CO_2 emission from the inland waters to the atmosphere (Cory et al., 2014), the overwheling majority of photo-degradation studies in the Arctic were conducted on oligotrophic lake waters and streams draining mineral soils of mountain regions (Ward and Cory, 2016; Cory et al., 2013, 2015). The dominance of photolytic processes in DOM processing in arctic waters was reported for N America (Cory et al., 2014; Ward et al., 2017), Canadian surface waters of the temperate zone (Winter et al., 2007; Porcal et al., 2013, 2014, 2015), and small Swedish humic-rich headwater catchments (Köhler et al., 2002). In contrast, several other studies from Scandinavia (Groeneveld et al., 2016; Koehler et al., 2014), Canada (Laurion and Mladenov, 2013; Gareis and Lesack, 2018) and NW Russia (Oleinikova et al., 2017; Chupakova et al., 2018)

demonstrated sizeable removal of colored (chromophoric DOM) but quite small (≤ 10%) impact of sunlight irradiation on bulk DOC concentration in streams, rivers and lakes. Note here that the interaction between photo- and bio-degradation is more important than the individual processes as photo-oxidation may transform DOM molecular structures into more bioavilable forms (e.g., Cory and Kling, 2018; Sulzberger et al., 2019).

Overall, available data demonstrate that an emerging paradigm on the importance of bio- and photodegradation may not be as consistent across the Arctic as previously thought, which call a need for further studies of these processes, encompassing wider range of aquatic settings. The numerous surface waters located within discontinuous to continuous permafrost zone of Northern Eurasia, where most aquatic systems are drained through frozen peat rather than mineral substrates, are poorly studied regarding bio- and photo-degradability of aquatic DOM. Yet, these regions (NE European Russia or Bolshezemelskaya tundra, Western Siberia Lowland, Northern Siberian Lowland, Kolyma and Yana-Indigirka Lowland) occupy > 2 million km² which is more than 10% of overall permafrost-affected land area and exhibit, in average, ten times higher concentration of soil organic C in the form of 0.5 to 3 m thick peat layer than the rest of the circumpolar regions (Tarnocai et al., 2009; Raudina et al., 2018). As a result of the dominance of histosols, the surface waters draining frozen peatlands are enriched in DOC compared to other permafrost-affected regions (Manasypov et al., 2014; Pokrovsky et al., 2015) and may provide disproportionally high contribution to overall DOM bio- and photo-degradability in the Arctic and subarctic regions.

Numerous experiments in permafrost-bearing and permafrost-free aquatic environments including both organic and mineral soil substrates relatively poor in DOC demonstrated that the headwater streams and soil leachate contain most bio-degradable and photo-degradable DOM (Ilina et al., 2014; Mann et al., 2014, 2015; Larouche et al., 2015; Spencer et al., 2015; Vonk et al., 2015). Photo-oxidation and biodegradation were also shown to play an important role in small

streams of temperate peatlands of UK and Scotland (Moody et al., 2013; Pickard et al., 2017; Dean et al., 2019). In the present study, we hypothesized that, given nutrient-poor nature of Sphagnum peat from histosols, the bioavailability of essentially recalcitrant DOM in surface waters of frozen peatlands will be low. However, we expected a gradient in the degree of bio- and photo-lability of DOM from permafrost subsidence, head water stream, thermokarst lake and large river, corresponding to the increase in water residence time (Mann et al., 2012).

To test these hypotheses, we used recommended standardized protocol for DOM biodegradation (Vonk et al., 2015) and applied it for 4 main aquatic components of a hydrological continuum 'permafrost subsidence → small stream → large thermokarst lake → large river (Pechora)'. We chose the largest frozen peatlands in Europe, the Bolshezemelskaya Tundra of NE European Russia which is represented by flat-mound (palsa) peat bog (discontinuous and continuous permafrost zone) and belongs to the watershed of the largest European permafrost-affected river, Pechora. Specific questions of this study were (*i*) to asses the difference in BDOC and photodegradable (PDOC) fraction of DOM in surface waters of frozen peat bog along the hydrological continuum, from permafrost depression to large rivers, (*ii*) to quantify the impact of temperature on biodegradation potential of surface waters from frozen peatbogs and predict possible impact of warming on DOM biodegradation efficiency, and (*iii*) to relate the BDOC and PDOC concentrations to the snapshot CO_2 concentration and emission.

2. Study site and methods

2.1. Geographical context and hydrological continuum of the Pechora River basin

The water samples were collected in the middle of July 2017 which is the middle summer period, consistent with time used by other researchers for biodegradation assays. The BolsheZemelskaya Tundra (BZT) peatland (continuous to discontinuous permafrost zone)

belongs to the Pechora River watershed (**Fig. S1)**, the largest European Arctic river draining permafrost-bearing terrain (watershed = 322,000 km²; mean annual discharge is 4140 m^3/s). The northern part of the Pechora watershed is covered by permafrost: discontinuous on the eastern part and sporadic to isolated on the western part (Brittain et al., 2009). The BZT is a hilly moraine lowland located between rivers Pechora and Usa (from the west and south) and the Polar Ural and Pai-Khoi ridge from the east. The dominant altitudes are between 100 and 150 m, created by hills and moraine ridges, composed of sands and silt with boulders. Between the moraines and ridges there are many lakes, mostly of thermokarst origin. The dominant soils are histosols of peat bogs and podzol-gleys in the southern forest-tundra zone. The mean annual temperature is -3.1°C and the mean annual precipitation is 503 mm. The dominant vegetation of the tundra zone is mosses, lichens and dwarf shrubs. Over past decades, the lakes of BZT exhibited sizeable increase in summer time temperature and pCO_2, presumably due to enhanced bacterial respiration of allochthonous DOM from thawing permafrost (Drake et al., 2019).

We sampled surface waters along the typical hydrological continuum shown in Fig. S1 and consisting of 1) depression in the moss and lichen cover of upland frozen peat bog, filled by water from thawing of ground ice (permafrost subsidence, 2.5 x 3 m size and 0.3 m depth); 2) small stream (~2 km length) originated from upland peat bog; 3) small thermokarst lake Isino (S_{area} = 0.005 km²) located within the peat bog, and 4) the Pechora River mainstream. Similar principle of the hydrological continuum was considered in the Kolyma River biodegradation experiments (Mann et al., 2012). The list of sampled water objects together with their physical, chemical, microbiological characteristics and parameters of CO_2 system is presented in **Table 1.** The surface waters were collected from the shore (depression and stream) or the PVC boat (r. Pechora and Lake Isino). The water samples were placed into 2-L Milli-Q pre-cleaned PVC jars and kept refrigerated until arrival to the laboratory, within 2-3 h after collection.

156 *2.2. Experimental set-up*

157 2.2.1. Biodegradation

158 For biodegradation assays we followed the standardized protocol for assessing
159 biodegradable DOC of Arctic waters (Vonk et al., 2015). To facilitate the implementation of
160 recommended protocol, we used exactly the same filter towers, inline filter holders, and vacuum
161 devices as depicted in Vonk et al. (2015). Initial samples were filtered through pre-combusted
162 (4.5 h at 450°C) Whatman GF/F filters of nominal poresize 0.7 µm. All the manipulations were
163 performed in laminar hood box (class A100) under sterile environment; the working space was
164 sterilized by UV light before preparation. Triplicate 30 mL aliquots of 0.7 µm-filtered water were
165 placed into pre-combusted (4.5 h at 450°C) dark borosilicate glass bottles of 40 mL volume
166 wrapped in Al foil to prevent any photolysis, without nutrient amendment and stored at 23±1°C
167 in the dark in thermostat. The bottles were closed with sterilized PVC caps. As recommended,
168 the caps were left loose and the bottles were shaken manually once a day avoiding the liquid
169 touching the cap. The incubated samples were re-filtered through pre-combusted 0.7 µm GF/F
170 filters using sterilized dismountable Sartorius 25 mm filter holder and a cleaned sterile syringe
171 after 0, 2, 7, 14 and 28 days of exposure. All handling and sampling of bottles was performed in
172 the laminar hood box under sterilized workspace. Filtered samples were acidified with 30 µL of
173 concentrated (8.1 M) double distilled HCl, tightly capped and stored in the refrigerator before
174 DOC analyses. Non-acidified portion of filtrate was used for pH, Specific Conductivity, DIC and
175 $UV_{254\,nm}$ and optical spectra measurement. Control runs were 0.22 µm sterile-filtered water which
176 was incubated in parallel to experiments and re-filtered through 0.7 µm GF/F filters at the day of
177 sampling.

178 In addition to this 'classic' protocol, we used alternative procedure of biodegradation
179 experiments to test maximally possible DOM removal by bacteria. For this, we replaced initial
180 0.7 µm GF/F filtration by 3 µm filtration through sterilized Nylon Sartorius membranes, to

increase the amount of bacterial cells capable to degrade DOM during incubation. The reason for that is that conventional 0.7 µm (GF/F) filtration might remove too many microbial cells (Dean et al., 2018). Besides, re-filtration through the same filter pore size (0.7 µm) recommended in classic protocol may not necessarily remove the newly formed microbial biomass as the cell size of bacteria grown during incubation may not exceed 0.7 µm. In this regard, initial 3 µm-filtration is equivalent of 100% inoculum used by Vonk et al. (2015) and can be considered as maximal enhancement of DOM biodegradation without addition of nutrients. Further, instead of 0.7 µm refiltration for sampling, we employed 0.22 µm filter pore size for DOC samplings during incubation. This allowed to remove all particulate organic carbon formed via microbial metabolism, as well as some newly grown microbial cells and therefore should enhance the degree of biodegradation calculated as the difference between initial 3 µm-filtration and 0.22 µm filtration at the date of sampling. The control runs were filtered through sterile 0.22 µm filters and incubated parallel to the experiments, following the standard approach for control abiotic experiments in incubation experiments (Köhler et al., 2002). They were re-filtered through 0.22 µm membrane at the day of experimental sampling. To insure the lack of DOC release from sterilized Nylon membrane, we run blank (Milli-Q) filtration through both 0.7 µm GF/F and 0.22 µm Nylon filters; in both cases the DOC blank was below 0.1-0.2 mg/L which is less than 1% of DOC concentration in our samples. The glass bottles were incubated in triplicates at 4±2°C, 22±1°C and 37±3°C using refrigerator and incubators and agitated manually at least once a day over 4 weeks of exposure.

2.2.2. Photodegradation

For photodegradation incubations, water samples of all sites except the river were collected in polypropylene jars and sterile filtered (0.22 µm Nalgene Rapid-Flow Sterile Systems) within 2 h of sampling and refrigerated. The filtrates were transferred under laminar

hood box into sterilized, acid-washed quartz tubes (150 mL volume, 20% air headspace) and placed at 3±2 cm depth into outdoor pool which was filled by river water having the light transparency similar to that of the Pechora River (1.5-2.0 m Secchi depth). In-situ measurements of sunlight intensity were conducted using submersible sunlight sensor. The outdoor pools were placed under unshaded area, at the latitude similar to that of the sampling sites. Slight wind movement and regular manual shaking allowed for sufficient mixing of the interior of reactors during exposure. All the experiments were run in triplicates. The water temperature was 19±3°C over 28 days of exposure (17 July - 14 August 2017), with an average magnitude of diurnal water temperature variation of 6°C (recorded every 3 h using EBRO EBI 20 Series loggers). The day light intensity was typically between 5,000 and 20,000 lux (in average 10,000 lux or 14±5 W/m^2) which is within the range of solar radiation at the latitude of the polar circle during this period of the year. Overall, we followed conventional methodology for photodegradation which is exposure of 0.2 µm-sterile filtered samples in quartz reactors in the outdoor pool (Vähätalo et al., 2003; Chupakova et al., 2018; Gareis and Lesack, 2018), solar simulator (Lou and Xie, 2006; Amado et al., 2014) or directly in the lake water (Laurion and Mladenov, 2013; Groeneveld et al., 2016). Note that the 0.22 µm sterile filtration is the only way of conducting photodegradation experiments, given that the autoclave sterilization of DOM-rich natural water would coagulate humic material and thus is not suitable (Andresson et al., 2018). We have chosen 4 week exposure time for consistency with biodegradation experiments described above and following the previous studies on photodegradation under sunlight, which is typically from 15 to 70 days (Moran et al., 2000; Vähätalo and Wetzel, 2004; Mostofa et al., 2007; Helms et al., 2008; Chupakova et al., 2018). Dark control experiments were conducted in duplicates, using sterilized glass tubes filled by sterile 0.22 µm-filtered water, wrapped in Al foil and placed in the same outdoor pool as the experiments. The headspace (approx. 20% of total reaction volume) was similar in experimental and control reactors. The individual reactors were sterile sampled at the

beginning and at the 2nd, 7th, 14th, 21th and 28th day of exposure. Each sampling sacrificed the entire reactor. The MilliQ blanks were collected and processed to monitor for any potential sample contamination introduced by our filtration, incubation, handling and sampling procedures. The organic carbon blanks of filtrates never exceeded 0.2 mg/L.

2.3. Analyses and treatment

The temperature, pH, O_2 and specific conductivity in surface waters were measured in the field as described previously (Shirokova et al., 2013b). Dissolved CO_2 concentration was measured using submersible Vaissala Carbocap® GM70 Hand-held carbon dioxide meter with GMP222 probes (accuracy 1.5%; see Serikova et al. (2018, 2019) for methodological details). The diffusional CO_2 flux was calculated using wind-based model (Cole and Caraco, 1998) with $k_{600} = 2.07 + 0.215 \times u_{10}^{1.7}$, where u_{10} is the wind speed at 10 m height. In the filtrates, we measured optical density at 254 nm and at selected wavelengths (365, 436, 465, and 665 nm) of the visible spectrum. The specific UV-absorbency ($SUVA_{254}$, L mg^{-1} m^{-1}) and E4:E6 ratios are used as a proxy for aromatic C, molecular weight and source of DOM (Weishaar et al., 2003; Peacock et al., 2013; Ilina et al., 2014).

The DOC and DIC were analyzed by high-temperature catalytic oxidation using TOC-VCSN, Shimadzu® (uncertainty ± 2%, 0.1 mg L^{-1} detection limit). The DIC was measured after sample acidification with HCl and DOC was analyzed in acidified samples after sparging it with C-free air for 3 min at 100 mL min^{-1} as non-purgable organic carbon (NPOC). Selected quartz reactors in photodegradation experiments were used to measure dissolved O_2 using Oxi 197i oximeter with a CellOx® 325 galvanic submersible sensor (WTW, Germany; ± 0.5% uncertainty). For this, the O_2 galvanic sensor was introduced into the quartz tube immediately after opening of the reactor and allowed to equilibrate for 5-10 min while protecting the open end of the tube from the exchange with atmospheric oxygen via wrapping it in Al foil. All filtered

sampled collected from photo-degradation experiments were acidified with ultrapure nitric acid and analyzed for major and trace elements following procedures employed in GET (Toulouse) for analyses of boreal humic waters (Oleinikova et al., 2017, 2018).

To account for possible microbial development in biodegradation experiments, we performed oligotrophic and eutrophic bacteria count in the course of incubation, following the standard methodology used in biodegradation experiments of peat waters (Stutter et al., 2013) as also decsribed previously (Shirokova et al., 2017b; Chupakova et al., 2018). In addition, we measured total bacterial number and quantified the dominant cell size morphology using DAPI fluorescence method (Porter and Feig, 1980). Control experiments did not demonstrate the presence of any countable cells in the observation fields.

The bio- and photodegradable DOC (BDOC and PDOC, respectively) were calculated in percent loss relative to control at each sampling time point *t* (0, 2, 7, 14 and 28 days) according to:

$$BDOC(\%)_t = 100\% \times (DOC_{t,\ control} - DOC_t)/DOC_{t,\ control} \quad (1)$$

Alternatively, the BDOC and PDOC were calculated in percent loss at time point *t* relative to the initial concentration of DOC ($DOC_{t=0}$) following Vonk et al. (2015):

$$BDOC(\%)_t = 100\% \times (DOC_{t=0} - DOC_t)/\ DOC_{t=0} \quad (2)$$

For most treatments and sampled waters, the difference between two methods of bio-/photodegradabale DOC concentration was statistically negligible. To assess the variability of results, shown as vertical uncertainties in the graphs, we used the percentage ratio of standard deviation of *n* replicates at the *i*-th day of exposure to the initial DOC concentration following:

$$SD_i = \sqrt{\frac{(BDOC_i^1 - BDOC_i^{mean})^2 + (BDOC_i^2 - BDOC_i^{mean})^2 + \ldots (BDOC_i^n - BDOC_i^{mean})^2}{n}} \quad (3)$$

$$\%SD_i = \frac{SD_i}{DOC_0} \cdot 100 \quad (4)$$

The results are presented as % $BOD_i \pm SD_i$.

To assess the uncertainties during photodegradation experiments, we used the percentage of standard deviation on *n* replicates at the *i*-th day of exposure to the DOC concentration in the dark (control) reactors as

$$PDOC_i^n = DOC_i^{blank} - DOC_i^n \quad (5)$$

$$PDOC_i^{mean} = \frac{PDOC_i^1 + PDOC_i^2 + \ldots PDOC_i^n}{n} \quad (6)$$

$$\%PDOC_i = \frac{PDOC_i^{mean}}{DOC_i^{blank}} \cdot 100 \quad (7)$$

$$SD_i = \sqrt{\frac{(PDOC_i^1 - PDOC_i^{mean})^2 + (PDOC_i^2 - PDOC_i^{mean})^2 + \ldots (PDOC_i^n - PDOC_i^{mean})^2}{n}} \quad (8)$$

$$\%SD_i = \frac{SD_i}{DOC_i^{blank}} \cdot 100 \quad (9)$$

The results are presented as % $PDOC_i \pm SD_i$

Note that in case of negative values provided by Eqn. 2, the BDOC was taken as 0% following the conventional practice in biodegradation experiments (Vonk et al., 2015). The uncertainties of BDOC % numbers were between ±5 and ±10% for experiments, at 4, 23 and 37°C using modified (3 μm and 0.22 μm filtration) protocol. In 'classic' protocol (0.7 μm GF/F filtration) the uncertainties were as high as 10-15% at the end of experiment. We believe that such high uncertainties are linked to high initial DOC concentration, triplicate measurements and simultaneous monitoring of experimental and control runs.

Statistical treatment included the least squares method and the Pearson correlation, because the data were normally distributed. The ANOVA method was used to test the differences in the average DOC concentration versus time in incubation experiments and in the controls and to assess the difference between the light experiments and the dark control for photo-degradation experiments. All calculations were performed in STATISTICA ver. 10 (StatSoft Inc.,Tulsa) at p = 0.05).

3. Results

3.1. Assessment of biodegradable DOC

The waters of hydrological continuum within the Pechora River basin are highly diverse (**Table 1**), with pH range from 3.8 (frozen peat depression) to 6.9 (r. Pechora). The soluble salts concentrations are low as the specific conductivity ranged from 20±10 µS cm^{-1} (stream, thermokarst lake) to ~60 µS cm^{-1} in the peat bog depression and the Pechora River. The DOC concentration decreased from 44 mg L^{-1} in frozen peat depression to ~8 mg L^{-1} in the Pechora River following the order of water residence time (flow direction) "depression >> stream ≥ thermokarst lake > r. Pechora". The DOC concentration was generally similar (within ± 2%) between 3, 0.7 and 0.22 µm pore size filtration of the initial sample, in agreement with former size fractionation measurement in Arctic and subarctic systems (Vasyukova et al., 2010; Pokrovsky et al., 2012, 2016). All sampled surface waters exhibited CO_2 supersaturation with respect to atmosphere (from 440 to 2400 ppm) and net CO_2 emission (diffusion) flux ranging from 34 to 74 mmol CO_2 m^{-2} d^{-1} (**Table 1**).

In both protocols of biodegradation experiments, two major features were noted: (1) the concentrations of 0.7 µm and 0.22 µm-filtered DOC did not decrease during the exposure and (2) there was no sizable (> 10%) difference between the control run and the incubation experiment (**Fig. 1)**. By 'classic' protocol of biodegradation experiments (0.7 µm GF/F filtration) at 23°C, the BDOC fraction ranged between 0 and 10 % for all surface waters. The modified procedure (3 µm initial filtration and 0.22 µm sampling) did not detect any significant biodegradation for any of the studied waters (average equaled to 5±5% at 4, 23 and 37°C, **Fig. 2 B, C, D**). The DIC concentrations remained constant (±5% of the initial value) in all experiments, but increased in stream water incubated at 37°C, where we measured ~10% increase over 28 days of exposure (not shown). This increase was equal to 0.2 mg/L of DIC. Note that equivalent decrease in DOC concentration could not be assessed, presumably due to instrument limitation

(the intrinsic uncertainty on NPOC analyses (ca. 2% of 15 mg/L of DOC) which did not allow measuring C change smaller than 0.3 mg/L.

The $UV_{254\,nm}$ absorbency of samples in the course of dark aerobic exposure demonstrated slight decrease with time (ca., between 5 and 10% over 28 days) in peat bog depression by 'classic' protocol (**Fig. S2** of **Supplement**). However, in all other treatments, the control was indistinguishable from experimental runs and the $SUVA_{254}$ remained constant within the uncertainties of triplicates (ca., ±5 to ±10%). Similarly, no measurable change in optical properties of DOM (absorbency at 365, 465, 665 nm and E4:E6 ratio) could be detected during exposition.

The microbial consortium of all systems was dominated by cocci (0.23 µm median size) and rods (0.96 x 0.20 µm) as revealed from DAPI fluorescent imaging. The number of culturable oligotrophic bacteria increased by a factor of ~ 100 after first 2-7 days of exposure at 22°C both in GF/F-filtered and 3µm-filtered samples, and then remained stable at ca. 10,000 to 20,000 CFU mL^{-1} till the end of experiments (**Fig. S3 A, C**). The highest concentration of oligotrophic bacteria was observed in the Pechora River, where as the other samples were not significantly different between each other. The CFU value at 4°C ranged between 1000 and 5000 CFU mL^{-1} and did not demonstrate any clear pattern with time of incubation (**Fig. S3 B**). The number of eutrophic bacteria ranged between 1,000 and 15,000 CFU mL^{-1} following the order: r. Pechora > stream ≥ peat bog depression ≥ thermokarst lake. There was no growth of eutrophic or oligotrophic bacteria at 37°C. The total cell number gradually increased in the course of experiment at 22°C (**Fig. S3 D**) with maximal changes observed in peatbog depression and the Pechora River (by a factor of 30 and 40, respectively). There was a progressive increase of rod-shaped bacillus relative to coccus in the Pechora River and a permafrost stream whereas the thermokarst lake and peatbog depression did no exhibit any systematic change in dominant bacteria morphologies during the biodegradation experiments. Note that the total cell number in surface waters of

354 Bolshezemelskaya Tundra were similar to those obtained in incubation experiments (see Table
355 1, Fig. S3).
356
357 *3.2. Photodegradation of DOM from frozen peatlands*
358 The pH of sunlight-exposed samples did not exhibit any systematic variation within 0.5
359 pH unit. The DIC remained fairly stable (within 0.5 mg/L) without any significant ($R^2 < 0.5$; $p > 0.05$) change during incubation, regardless of the type of system, DOC and DIC concentration
360
361 (not shown). The exposed water remained oxygenated (average O_2 saturation close to 90%) with
362 no detectable change (i.e. > 10%) over the course of experiment. Specifc conductivity also
363 remained highly stable over full period of exposure.
364 The bacteria count in photo-degradation reactors at the beginning of exposure and after
365 14 and 28 days of incubation yielded between 1 and 100 CFU mL^{-1}. This is a factor of 100 to
366 1000 lower than the number of cells in experiments of bio-degradation run in non-sterilized
367 waters over the same duration of experiments (section 3.1). As such, the microbial degradation
368 was considered negligible at our experimental conditions of sunlight exposure.
369 There was no sizeable decrease in DOC concentration during 28 d of exposure to sunlight
370 (**Fig. 3 A**). This relative change of DOC concentration ranged from -5 % to +5 % and it did not
371 exceed the non-systematic variability among triplicates. Although the triplicate agreed within
372 less than 2 % (the symbol size in **Fig. 3**), the small change of DOC in peat depression was similar
373 in light experiment and dark control. The % PDOC (relative to starting solution) as a function of
374 exposure time over 28 days of experiment ranged from 0 to 5% in peatbog depression and 0 to
375 10% in thermokarst lake and permafrost spring (**Fig 3 B**).
376 The $SUVA_{254\ nm}$ in photodegradation experiments decreased much stronger than the
377 DOC. The SUVA decrease relative to control was mostly pronounced in permafrost stream (**Fig.**
378 **4**). The optical properties of DOC demonstrated sizeable decrease of E_{365}/E_{470} ratio

corresponding to UV/vis absorbing functional groups (**Fig. S4 A),** which was consistent with decreasing $SUVA_{254\ nm}$ during sunlight exposure. The E_{254}/E_{436} ratio, corresponding to autochthonous vs. terrestrial DOM, did not demonstrate any sizeable change over the course of experiment **(Fig. S4 B).**

Most of major and trace elements did not show any significant (at $p < 0.05$) change in concentration over the photodegradation experiments. Only a few nutrients (P, Fe, Zn, B) and trace metals (Zn, Ti, V, Zr, Nb and Th) demonstrated a decrease in concentration. The decrease of Fe was mostly pronounced in permafrost stream, and did not occur in permafrost depression (**Fig. 5 A**) whereas total dissolved phosphorus systematically decreased, by 20 to 50%, over 28 days of sunlight exposure in permafrost depression, thermokarst lake and permafrost stream (**Fig. 5 B**). A decrease of Ti, Zn, Nb and Th also occurred in thermokarst lake and permafrost stream (not shown). Overall, the magnitude of decrease of P, Fe, Ti, V and Zn in photodegradation experiments followed the order "permafrost stream > thermokarst lake > permafrost depression".

4. Discussion

4.1. High stability of dissolved organic matter to biodegradation in surface waters from frozen peatland

The unexpected result of this study was very low BDOC fraction, measured not only in large river (Pechora) but also in small stream, thermokarst lake and peatland depressions formed due to permafrost subsidence. According to compilation of available biodegradation studies, the BDOC fraction (28 days of exposure) ranges from 3 to 18% (mean 13%) in waters of continuous permafrost zone and from 5 to 15% (mean 14%) in discontinuous permafrost zone (Vonk et al., 2015). This is higher than the 0 to 10 % of BDOC measured for all water objects from the discontinuous permafrost zone in this study. Note that very few biodegradability studies in aquatic systems dealt with frozen peatlands, and all previous incubation experiments used water

404 from mountainous regions on mineral soils in Scandinavia, Alaskan slope and Canada, yedoma
405 regions of Eastern Siberia, or the Yenisey basin. Only one former biodegradation study in peat
406 mire context demonstrated sizable bioavailability of soil leachate to lake water bacteria (Roehm
407 et al., 2009), but this work did not deal with pure aquatic endmember, unlike this study. Instead,
408 the BDOC of frozen peatlands surface waters measured for the Bolshezemelskaya Tundra inland
409 waters was comparable with the value suggested by Vonk et al (2015) for non-permafrost aquatic
410 DOC (0-1 %).

411 Another important point revealed in previous work on biodegradation of Arctic waters is
412 that aquatic BDOC in large streams and rivers decreased as the Arctic summer progressed (Vonk
413 et al., 2015), although this pattern was absent for soil leachates and small streams. In our case,
414 thermokarst lake Isino and r. Pechora can be considered as sufficiently large hydrological
415 systems. The sampling was performed in the end of July which is already summer baseflow
416 period and as such 0 to 5 % biodegradable DOC measured for Isino and Pechora in this study is
417 comparable with 0 to 20% BDOC loss reported in large streams and rivers at ~200 Julian day
418 (Vonk et al., 2015). However, small stream and permafrost subsidence remain clearly at the very
419 low edge of BDOC % lost reported for soils and streams in summer. In the estuarine zone of
420 largest European Arctic permafrost-free river, Severnaya Dvina, there was no measurable
421 biodegradation in spring, when the DOM was dominated by allochthonous sources, but a 15 to
422 20% decrease of DOC occurred during first 300 h in river water collected in August, when
423 sizeable phytoplankton productivity was observed (Shirokova et al., 2017b). In laboratory
424 experiments with individual cultures, moss and peat leachates were also sizably biodegraded over
425 1-2 days of exposure (Shirokova et al., 2017a), whereas the same bacterial species were not
426 capable degrading DOM from surface waters draining peatland and moss covered bogs
427 (Oleinikova et al., 2018). Following a recommended protocol of biodegradation assays (Vonk et
428 al., 2015), in this work we incubated natural water without nutrients. This creates potential bias

for application of obtained results to various subarctic settings. For example, one should note that nutrients and labile DOM addition downstream (away from the oligotrophic bogs) can increase the capacity of bio-degradation and related CO_2 emission in large river, before its discharge to the Arctic Ocean. Further, it is possible that in natural settings, the input of biolabile DOC from terrestrial vegetation may enhance the bioavailability of stable DOC (e.g., Textor et al., 2018) although this effect could not be tested in this study.

Mechanistic reasons for extremely low bioavailability of DOC from studied peatlands remain unclear and require in-depth analysis of DOM molecular structure and stoichiometry as well as high resolution microbial approaches. It is known that the DOM released from frozen soils contains high proportions of biologically labile protein-like and photochemically reactive aromatic substances (Gao et al., 2018). Following the pioneering study of Ward et al. (2017), we hypothesize that, similar to DOC from organic (non-permafrost) layer, the concentration of high-lability, aliphatic-like DOC in surface waters of frozen peatlands is too low to sustain microbial population, or that this aquatic DOC, remaining after microbial processing of soil porewater DOC is of low lability for microbes capable to degrade aliphatic-like DOC and inhabiting aerobic zone of permafrost surface waters. The constant pattern of UV_{254} absorbency in biodegradation experiment was consistent with negligible change in BDOC over 28 days of incubation. In comparison, the biodegradation of peat water from European boreal zone was associated with an increase in SUVA by up to 7.4 %, which also implies an increase in the proportion of aromatic compounds (Hulatt et al., 2014). The total bacterial number in studied surface waters $(0.5\text{-}5)\times10^6$ cell mL^{-1} is in excellent agreement with other studies of thermokarst peatland lake waters (Deshpande et al., 2016). Following these researchers, we suggest that the reason of low biodegradability of peatland humic waters is that the majority of active bacteria are associated with particles (> 3 μm) rather than present as free-living cells (< 1 μm) capable to DOC processing. In addition, the bacterial communities are not just shaped by size fractionation

by filtration, but also the presence or absence of bacterial grazers (Dean et al., 2018). However, further mechanistic studies of model aquatic bacterial communities capable to affect the degradation of DOM from different terrestrial sources are necessary (Logue et al., 2016).

Interestingly, there was no measurable difference in BDOC at 4, 23 and 37°C, as the proportion of BDOC at all temperatures for each system was below 5-10%. This result allows preliminary prediction of possible consequence of climate change and surface water heating in high latitudes. In a short-term climate warmings scenario, or assuming fast heating of surface waters due to prolonged heat wave of draught occurring both in European, permafrost-free (Shirokova et al., 2013a) and western Siberian (Pokrovsky et al., 2013) permafrost-bearing peatlands, we do not foresee any measurable change in biodegradability of DOM from the water column. Under even most extreme heating scenario of thermokarst lakes, river and depressions of the frozen peatland territories, the short-term bio-processing of aquatic DOM may remain close to zero.

4.2. Negligible impact of photodegradation on DOM transformation in inland waters of frozen peatlands

The second main result of this work was high stability of surface waters DOM to sunlight exposure. Over 28 d of incubation in outdoor pools at the conditions corresponding to surface (< 0.05 m depth) water layer of thermokarst lakes and streams from permafrost zone, the change in DOC concentration was less than 5-10% of the initial value and was not distinguishable from that in the dark control (**Fig. 3 A, B**). Therefore, the DOM of all frozen peatland is quite refractory and not subject to measurable photodegradation over 4 weeks of exposure. This period is comparable with the water residence time in small depressions of frozen peatlands (Novikov et al., 2009) and small thermokarst thaw ponds of frozen palsa peatbogs (Manasypov et al., 2015) but much higher than the water travel time in small streams (< 10 km long) and in the lower

reaches of Pechora river, from the site of sampling till the Arctic Ocean (ca. several days). This result apparently contradicts the recent paradigm that the photochemical oxidation may account for 70 to 95% of total DOC processed in the water column of arctic lakes, rivers and soils (Cory et al., 2013, 2014; Ward and Cory, 2016; Ward et al., 2017). However, the conclusion of this group of authors is based on study of distilled water leachates of mineral soils, headwater streams, fresh permafrost thaw sites and lakes of N. Alaska slopes, developed on mineral substrates. In contrast, the results of DOM photolysis in polygonal and runnel ponds located in frozen peatlands (2 m peat, 40-60 cm active layer thickness) of continuous permafrost regions (Canada High Arctic) demonstrated a relatively fast decay of water color and fluorescence, but insignificant losses of DOC over 12 days of exposure time (Laurion and Mladenov, 2013). Recently, no measurable photochemical loss of ancient permafrost DOC has been revealed in the thawing yedoma permafrost sites of the Kolyma River, its tributaries and streams (Stubbins et al., 2017). Another recent study of DOM photodegradation in boreal high-latitude peatland streams of the White Sea watershed demonstrated only 10% decrease in DOC concentration over 10 days of incubation under sunlight (Oleinikova et al., 2017). In the estuarine zone of the largest European Arctic river draining wetland- and forest-dominated permafrost-free territory (Severnaya Dvina), we did not find any measurable photo-degradation of DOM over 1 month of exposure (Chupakova et al., 2018). This comparison clearly demonstrates highly contrasting DOM photolability between the aquatic systems of N. America, draining through mineral soil substrates, and that of boreal and subarctic peatlands.

Further, due to high homogeneity of organic substrate surrounding studied waters and similar allochthonous origin of DOM in all surface waters of frozen peatlands, there was no dramatic difference in DOM photodegradability over the hydrological continuum in NE European Arctic, which also contrasts the results obtained in aquatic systems on mineral soils (Cory et al., 2007, 2013; Reader et al., 2014). It is possible that either 1) photochemical

degradation of humic peat waters occurs very fast, during first hours to days upon their exposure to sunlight or 2) that the nature of DOM is so refractory that much longer exposure periods, on the order of several months to years (as in the Arctic coast) are necessary to photodegrade the DOM from frozen peatlands. The first explanation is consistent with recent experiments on photodegradation of fresh peat mire water, collected in taiga region of NW Russia, where about 50% of bogwater DOC was photodegraded over 2 days of exposure to sunlight (Oleinikova et al., 2017).

As such, it is possible that all surface waters sampled for experiments in this study, including stagnant water in permafrost depression, have already contacted with sunlight for more than several days and thus became photo-resistant. Assuming the maximal possible DOC loss due to photolysis assessed in our experiments (0.1 mg C L^{-1} d^{-1} corresponding to a loss of 3 mg/L during 28 days) and the light penetration depth of 0.5 m which is comparable with the typical depth of studied water bodies, the photodegradation can contribute to less than 10 % of total CO_2 emission flux from the water surfaces of frozen peatlands (0.4-0.8 g C m^{-2} d^{-1} in this work; 0.8 to 4.4 C m^{-2} d^{-1} in western Siberian rivers and streams, located on very similar context of frozen peat bogs, Serikova et al., 2018). The maximal PDOC value measured in this work is also at the lower end range of DOM photodegradation contribution to C flux in North European boreal and subarctic settings. Thus, DIC annual photo-production contributed between 1 and 8 % of CO_2 emissions from a humic lake in south of Sweden (Groeneveld et al., 2016) and globally in the boreal and subarctic zone, sunlight-induced CO_2 emissions represent about one tenth to the CO_2 emission from lakes and reservoirs (Koehler et al., 2014).

The evolution of optical properties of DOM as a function of exposure time in different samples was consistent with the mechanisms of photo-sensitive DOM removal during irradiation. The ratio E_{365}/E_{470} is known to correlate with the degree of condensation of DOM aromatic groups and with the degree of humification (Chin et al., 1994; Hur et al., 2006) whereas UV_{254}

529 is used as proxy for aromatic C and source of DOM (Chen et al., 1977; Uyguner and Bekbolet,
530 2005). The optical properties of DOC were much less conservative under sunlight exposure
531 compared to total dissolved C concentration, as $UV_{254\ nm}$ and E_{365}/E_{470} ratio sizably decreased in
532 the course of experiments. Numerous studies of allochthonous riverine DOM also revealed that
533 photodegradation of colored DOM (CDOM) and $SUVA_{254}$ were much greater than DOC losses
534 (Spencer et al., 2009; Reche et al., 2000; Vähätalo and Wetzel, 2004; Mostofa et al., 2011; Bittar
535 et al., 2015; Gareis and Lesack, 2018). A decrease of E_{365}/E_{470} corresponded to removal of UV
536 rather than visual light absorbing functional groups, whereas a constant pattern of E_{254}/E_{436} ratio
537 within the hydrological continuum 'depression → stream → lake → river' was consistent with
538 lack of autochthonous DOM in all studied water objects, which were dominated by terrestrial
539 (aromatic) DOM from peat horizons. Overall, our observations confirm the conclusion achieved
540 from a recent compilation of available data across the world that degradation processes act
541 preferentially on CDOM rather than DOC concentration (Massicotte et al., 2017; Oleinikova et
542 al., 2017).

543 In contrast to DOC, sizeable removal of dissolved P and Fe together with some related
544 trace elements (Ti, V, Zn, Nb) during photolysis of surface waters reflects transformation and
545 coagulation of Fe-rich colloids, that behave independent on organic colloids in humic waters
546 (Vasyukova et al., 2010; Pokrovsky et al., 2016). This precipitation of Fe hydroxides together
547 with P and insoluble trace elements was mostly pronounced in permafrost stream which had the
548 highest pH. In this stream, Fe(III) hydroxide was not stable due to pronounced hydrolysis. After
549 photolytic removal of small amount of DOM that stabilized colloidal Fe (Oleinikova et al., 2017),
550 Fe hydroxide could coagulate and coprecipitate P and some trace elements.

551

552

553 *4.3. Lack of bio- and photodegradation in humic surface waters of frozen peat bogs*
554 *despite sizeable CO_2 emission*

555 The main result of the present study is that, despite well-known supersaturation of lentic
556 and lotic waters of frozen peatlands to atmospheric pCO_2 (Serikova et al., 2018, 2019), these
557 waters exhibit negligible bio- and photo-degradability over time scale (28 days) comparable with
558 or exceeding the water residence time in various reservoirs. For consistency with other studies in
559 high latitudes, we assessed the bio-and photodegradability of DOM during middle summer
560 period. Non-accounting for the spring freshet, which represents more than 60% of annual DOM
561 transport in similar boreal and subarctic rivers of European Russia (Pokrovsky et al., 2010) and
562 western Siberia (Pokrovsky et al., 2015; Vorobyev et al., 2019), may create substantial bias when
563 extending our results to other territories of the subarctic during full open water period. However,
564 it was recently shown that during spring flood, the DOM in the largest European Arctic River,
565 Severnaya Dvina, which is similar to the Pechora River, is not at all biodegradable (Shirokova et
566 al., 2017b). Moreover, the spring-time period does not exhibit any particularly high C
567 concentrations in thaw ponds and thermokarst lake waters of frozen peatlands (Manasypov et al.,
568 2015), and CO_2 emissions from rivers and lakes of permafrost-affected wetlands of western
569 Siberia were not much higher in spring compared to other seasons (Serikova et al., 2018, 2019).
570 Therefore, although our seasonally-restricted data set is not representative for the pan Arctic
571 environment and further studies with high spatial resolution across different climate zones are
572 needed (see examples in Lapierre and del Giorgio, 2014), our findings are at odds with the
573 dominant paradigm that bio- and photodegradation control the DOC removal from arctic aquatic
574 ecosystems (Abbot et al., 2014; Cory et al., 2014; Spencer et al., 2015). Given incontestable bio-
575 and photodegradability of peat pore waters and frozen soil extracts reported across the Arctic
576 (Vonk et al., 2015; Selvam et al., 2017), this strongly suggests that the DOM that arrives to small
577 rivers and even permafrost depressions via lateral peat soil outflux is already highly degraded.

578 This is consistent with general idea that rates of DOM photochemical alteration and rates of
579 microbial responses to altered DOM are typically rapid, from minutes to days (Cory and Kling,
580 2018). As such, the majority of elevated CO_2 measured in surface waters of permafrost peat
581 landscape originates from degradation of soil water DOM once it enters open surface water. This
582 is especially true for photo-oxidation, which is not likely to occur in the soil.

583 We believe that the degradation of soil DOM in surface waters of frozen peatlands occurs
584 very fast and completes within first hours or days. This is shorter than the residence time of water
585 in permafrost depressions, thaw ponds and rivers (Manasypov et al., 2015). As a result, we did
586 not detect sizeable bio- and photodegradation of residual DOM in various types of inland waters
587 from permafrost landscapes. In order to explain persistent CO_2 supersaturation of inland waters
588 from peatlands, we suggest that benthic respiration of stream, lake and river sediments produce
589 sizeable amount of CO_2 thus increasing overall C emission potential of the aquatic systems
590 (MacIntyre et al., 2018; Valle et al., 2018). For example, anaerobic C mineralization of
591 thermokarst lake sediments is fairly well established in discontinuous permafrost zone of peat
592 bogs in western Siberia (Audry et al., 2011) and Canada (Deshpande et al., 2017). Note that the
593 potential for dark DOM chemical oxidation in iron-rich organic-rich waters facing redox
594 oscillation (i.e., Page et al., 2012) is rather low in studied thermokarst waters which remain
595 essentially oxic over full depth of the water column during unfrozen period of the year.

596 The findings of this study and widely reported dominance of non-biodegradable DOC (0-
597 1% BDOC) in large rivers and streams of the non-permafrost zone (Vonk et al., 2015) suggest
598 that 1) the majority of BDOC is degraded before its arrival to large aquatic reservoirs, and 2) the
599 CO_2 supersaturation and emission of surface waters from frozen peatlands is due to soil pore
600 water and sediment respiration rather than aerobic bio- and photo-degradation of DOM in the
601 water column. Further, the non-increase in BDOC fraction during temperature rise from 4 to
602 37°C implies that, within the climate warming scenario, the heating of peat surface waters will

603 be a minor factor of overall CO_2 balance. Instead, the change of water path and residence time in
604 pore waters of frozen peatlands, the rate of supra-permafrost water delivery, and the magnitude
605 of benthic respiration in large rivers and thermokarst lakes may control the CO_2 emission from
606 inland waters.
607
608 **Conclusions**
609 This work revealed high resistance of surface waters collected in permafrost peatland to
610 both bio- and photo-degradation. Less than 5-10% of the initial aquatic DOC was removed over
611 1 month of dark aerobic incubation at 4, 22 and 37°C as well as during sunlight exposure of
612 sterile-filtered waters. In contrast to expected differences in bio- and photo-lability between small
613 permafrost subsidences, streams, large lake and the Pechora River, there was no measurable
614 difference in surface waters BDOC concentration along the hydrological continuum. The
615 contribution of aerobic DOM biodegradation within the water column to observed CO_2
616 supersaturations and net CO_2 emission fluxes from bog water, lakes, streams and rivers of
617 peatland territories located within discontinuous permafrost zone is less than 10%. Despite
618 decrease in CDOM during photolysis, this process does not significantly contribute to total DOC
619 degradation and C emission from the surface of inland waters of frozen peatlands.
620 We hypothesize that refractory nature of DOM from frozen peatlands which is already
621 processed in soil waters before arriving to lentic and lotic surface reservoirs create unfavorable
622 conditions for biodegradation. The reason for high stability of DOM from frozen peatland to
623 photolysis is less clear but can be linked to fast photo-degradation of peat bog and soil shallow
624 underground) waters after their exposure to the surface, occurring within the first hours to days.
625 We conclude on negligible impact of separate bio- and photo-degradation on DOM processing
626 and CO_2 emission in surface waters of frozen peatlands. This calls for future work to quantify

the combined bio- and photo-lability of peat pore waters, thawing soil ice, and suprapermafrost flow, which deliver the DOM to the rivers, lakes and depressions.

Acknowledgements

This work was supported by RFFI (RFBR) grants No 17-05-00348_a and 17-05-00342_a, Program FANO No 0409-2015-0140, RFFI No 18-05-01041 and UroRAN No 18-9-5-29. Additional funding from JPI Climate initiative, financially supported by VR (the Swedish Research Council) grant no. 325-2014-6898, is also acknowledged.

References

Abbott, B. W., Larouche, J. R., Jones, J. B., Bowden, W. B., and Balser, A. W.: Elevated dissolved organic carbon biodegradability from thawing and collapsing permafrost, J. Geophys. Res., 119, 2049–2063, 2014.

Amado, A. M., Cotner, J. B., Cory, R. M., Edhlund, B. L., and McNeill, K.: Disentangling the interactions between photochemical and bacterial degradation of dissolved organic matter: amino acids play a central role, Microb. Ecol., 69(3), 554-566, 2014.

Andersson, M. G. I., Catalán, N., Rahman, Z., Tranvik, L. J., and Lindström, E. S.: Effects of sterilization on dissolved organic carbon (DOC) composition and bacterial utilization of DOC from lakes, Aquat. Microb. Ecol., 82, 199-208, 2018.

Ask, J., Karlsson, J., and Jansson, M.: Net ecosystem production in clear-water and brown-water lakes, Glob. Biogeochem. Cycles, 26, GB1017, doi:10.1029/2010GB003951, 2012.

Audry, S., Pokrovsky, O. S., Shirokova, L. S., Kirpotin, S. N., and Dupré, B.: Organic matter mineralization and trace element post-depositional redistribution in Western Siberia thermokarst lake sediments, Biogeosciences, 8, 3341-3358, 2011.

Berggren, M., Laudon, H., Haei, M., Ström, L., and Jansson, M.: Efficient aquatic bacterial metabolism of dissolved low-molecular-weight compounds from terrestrial sources, ISME J., 4, 408-416, 2010.

Bittar, T. B., Vieira, A. A. H., Stubbins, A., and Mopper, K.: Competition between photochemical and biological degradation of dissolved organic matter from the cyanobacteria *Microcystis aeruginosa*, Limnol. Oceanogr., 60, 1172-1194, 2015.

Brittain, J. F., Gıslason, G. M., Ponomarev, V. I., Bogen, J., Jensen, A. J., Khokhlova, L. G., Kochanov, S. K., Kokovkin, A. V., Melvold, K., Olafsson, J. S., Pettersson, L.-E., and Stenina, A. S.: Arctic Rivers (chapter 9), pp. 337-379. In: Rivers of Europe, Eds: Tockner K., Uehlinger U., Robinson C.T., Academic Press Elsevier, 2009.

Chen, Y., Senesi, N., and Schnitzer, M.: Information provided on humic substances by E4/E6 ratios, Soil Sci. Soc. Amer. J., 41, 352-358, 1977.

Chin, Y.-P., Aiken, G., and O'Loughlin, E.: Molecular weight, polydispersity, and spectroscopic properties of aquatic humic substances. Environ. Sci. Technol., 28, 1853-1858, 1994.

Chupakova, A. A., Chupakov, A. V., Neverova, N. V., Shirokova, L. S., and Pokrovsky, O. S.: Photodegradation of river dissolved organic matter and trace metals in the largest European Arctic estuary. Sci. Total Environ., 622–623, 1343–1352, 2018.

Cole, J. J. and Caraco, N. : Atmospheric exchange of carbon dioxide in a low-wind oligotrophic lake measured by the addition of SF6. Limnol. Oceanog., 43, 647–656, 1998.

Cory, R. M., McKnight, D., Chin, Y. P., Miller, P., and Jaros, C. L.: Chemical characteristics of fulvic acids from Arctic surface waters: Microbial contributions and photochemical transformations, J. Geophys. Res., 112, G04S51, doi:10.1029/2006JG000343, 2007.

Cory, R. M., Crump, B. C., Dobkowski, J. A., and Kling, G. W.: Surface exposure to sunlight stimulates CO_2 release from permafrost soil carbon in the Arctic, Proc. Natl. Acad. Sci. USA, 110(9), 3429-3434, 2013.

Cory, R. M., Ward, C. P., Crump, B. C., and Kling, G. W.: Sunlight controls water column processing of carbon in arctic fresh waters, Science, 345, 925-928, 2014.

Cory, R. M., Harrold, K. H., Neilson, B. T., Kling, G. W.: Controls on dissolved organic matter (DOM) degradation in a headwater stream: the influence of photochemical and hydrological conditions in determining light-limitation or substrate-limitation of photo-degradation, Biogeosciences, 12, 6669–6685, 2015.

Cory, R. M., Kling, G. W.: Interactions between sunlight and microorganisms influence dissolved organic matter degradation along the aquatic continuum, Limnol. Oceanogr. Lett., 3, 102–116, 2018.

Dean, J. F., van Hal, J. R., Dolman, A. J., Aerts, R., and Weedon, J. T.: Filtration artefacts in bacterial community composition can affect the outcome of dissolved organic matter biolability assays, Biogeosciences, 15, 7141-7154, https://doi.org/10.5194/bg-15-7141-2018, 2018.

Dean, J. F., Garnett, M. H., Spyrakos, E., Billett, M. F.: The potential hidden age of dissolved organic carbon exported by peatland streams, J. Geophys. Res.: Biogeosciences, 124, 328–341, 2019.

Deshpande, B. N., Maps, F., Matveev, A., and Vincent, W. F., 2017. Oxygen depletion in subarctic peatland thaw lakes, Arctic Science, 3(2), 406-428, 2017.

Deshpande, B. N., Crevecoeur, S., Matveev, A., and Vincent, W. F.: Bacterial production in subarctic peatland lakes enriched by thawing permafrost, Biogeosciences, 13, 4411-4427, 2016.

Drake, T. W., Holmes, R. M., Zhulidov, A. V., Gurtovaya, T., Raymond, P. A., McClelland, J. W., and Spencer, R. G. M.: Multidecadal climate-induced changes in Arctic tundra lake geochemistry and geomorphology, Limnol. Oceanogr., 64, S179-S191, 2019.

Gao, L., Zhou, Z., Reyes, A. V., and Guo, L.: Yields and characterization of dissolved organic matter from different aged soils in northern Alaska, J. Geophys. Res.: Biogeosciences, 123, 2035–2052, 2018.

Gareis, J. A. L., and Lesack, L. F. W.: Photodegraded dissolved organic matter from peak freshet river discharge as a substrate for bacterial production in a lake-rich great Arctic delta, Arctic Science, 4(4), 557-583, 2018.

Groeneveld, M., Tranvik, L., Natchimuthu, S., and Koehler, B.: Photochemical mineralisation in a boreal brown water lake: considerable temporal variability and minor contribution to carbon dioxide production, Biogeoscience, 13, 3931-3943, 2016.

Helms, J. R., Stubbins, A., Ritchie, J. D., Minor, E. C., Kieber, D. J., Mopper, K.: Asorption spectral slopes and slope ratios as indicators of molecular weight, source, and photobleaching of chromophoric dissolved organic matter, Limnol. Oceanogr., 53(3), 955-969, 2008.

Holmes, R. M., McClelland, J. W., Raymond, P. A., Frazer, B. B., Peterson, B. J., and Stieglitz, M.: Lability of DOC transported by Alaskan rivers to the Arctic Ocean, Geophys. Res. Lett., 35, L03402, doi:10.1029/2007GL032837, 2008.

Hulatt, C. J., Kaartokallio, H., Asmala, E., Autio, R., Stedmon, C. A., Sonninen, E., Oinonen, M., and Thomas, D. N.: Bioavailability and radiocarbon age of fluvial dissolved organic matter (DOM) from a northern peatland-dominated catchment: effect of land-use change, Aquat. Sci., 76(3), 393-404, 2014.

Hur, J., Williams, M. A., and Schlautman, M. A.: Evaluating spectroscopic and chromatographic techniques to resolve dissolved organic matter via end member mixing analysis, Chemosphere, 63, 387-402, 2006.

Ilina, S. M., Drozdova, O. Yu., Lapitsky, S. A., Alekhin, Yu. V., Demin, V. V., Zavgorodnaya, Yu. A., Shirokova, L. S., Viers, J., and Pokrovsky, O. S.: Size fractionation and optical properties of dissolved organic matter in the continuum soil solution-bog-river and terminal lake of a boreal watershed, Org. Geochem., 66, 14–24, 2014.

Kaiser, K., Canedo-Oropeza, M., McMahon, R., and Amon, R. M. W.: Origins and transformations of dissolved organic matter in large Arctic rivers, Sci. Reports, 7, 13064, 2017.

Karlsson, J., Jansson, M., and Jonsson, A.: Respiration of allochthonous organic carbon in unproductive forest lakes determined by the Keeling plot method, Limnol. Oceanogr., 52, 603-608, 2007.

Koehler, B., Landelius, T., Weyhenmeyer, G. A., Machida, N., and Tranvik, L.J.: Sunlight-induced carbon dioxide emissions from inland waters, Global Biogeochem. Cycles, 28, 696–711, 2014.

Köhler, S., Buffam, I., Jonsson, A., and Bishop, K.: Photochemical and microbial processing of stream and soil water dissolved organic matter in a boreal forested catchment in northern Sweden, Aquat. Sci., 64, 269–281, 2002.

Lapierre, J.-F., Guillemette, F., Berggren, M., and del Giorgio, P. A.: Increases in terrestrially derived carbon stimulate organic carbon processing and CO_2 emissions in boreal aquatic ecosystems, Nature Comm., 4, 2972, doi:10.1038/ncomms3972, 2013.

Lapierre, J.-F. and del Giorgio, P. A.: Partial coupling and differential regulation of biologically and photochemically labile dissolved organic carbon across boreal aquatic networks, Biogeosciences, 11, 5969-5985, https://doi.org/10.5194/bg-11-5969-2014, 2014.

Larouche, J. R., Abbott, B. W., Bowden, W. B., Jones, and J. B.: The role of watershed characteristics, permafrost thaw, and wildfire on dissolved organic carbon biodegradability and water chemistry in Arctic headwater streams, Biogeosciences, 12, 4221-4233, 2015.

Laurion, I., and Mladenov, N.: Dissolved organic matter photolysis in Canadian Arctic thaw ponds, Environ. Res. Lett., 8, 035026, doi.org/10.1088/1748-9326/8/3/035026, 2013.

Logue, J. B., Stedmon, C. A., Kellerman, A. M., Nielsen, N. J., Andersson, A. F., Laudon, H., Lindström, E. S., and Kritzberg, E. S.: Experimental insights into the importance of aquatic bacterial community composition to the degradation of dissolved organic matter, ISME J., 10, 533–545, 2016.

Lou, T., and Xie, H.: Photochemical alteration of the molecular weight of dissolved organic matter, Chemosphere, 65, 2333-2342, 2006.

MacIntyre, S., Cortes, A., and Sadro, S: Sediment respiration drives circulation and production of CO_2 in ice-covered Alaskan arctic lakes, Limnol. Oceanogr. Lett., 3, 302–310, 2018.

Manasypov, R. M., Pokrovsky, O. S., Kirpotin, S. N., Shirokova, L. S.: Thermokarst lake waters across permafrost zones of Western Siberia, Cryosphere 8, 1177-1193, 2014.

Manasypov, R. M., Vorobyev, S. N., Loiko, S. V., Kritzkov, I. V., Shirokova, L. S., Shevchenko, V. P., Kirpotin, S. N., Kulizhsky, S. P., Kolesnichenko, L. G., Zemtzov, V. A., Sinkinov, V. V., and Pokrovsky, O. S.: Seasonal dynamics of organic carbon and metals in thermokarst lakes from the discontinuous permafrost zone of western Siberia, Biogeosciences, 12, 3009-3028, 2015.

765 Mann, P. J., Davydova, A., Zimov, N., Spencer, R. G. M., Davydov, S., Bulygina, E., Zimov, S.,
766 Holmes, R. M.: Controls on the composition and lability of dissolved organic matter in
767 Siberia's Kolyma River basin, J. Geophys. Res., 117, G01028, doi: 10.1029/2011JG001798,
768 2012.
769 Mann, P. J., Sobczak, W. V., LaRue, M. M., Bulygina, E., Davydova, A., Vonk, J. E., Schade,
770 J., Davydov, S., Zimov, N., Holmes, R. M., Spencer, R. G. M.: Evidence for key enzymatic
771 controls on metabolism of Arctic river organic matter, Global Change Biol., 20(4), 1089-
772 1100, 2014.
773 Mann, P. J., Eglinton, T. I., Mcintyre, C. P., Zimov, N., Davydova, A., Vonk, J. E., Holmes, R.
774 M., Spencer, R. G. M.: Utilization of ancient permafrost carbon in headwaters of Arctic
775 fluvial networks, Nat. Commun., 6, doi: 10.1038/ncomms8856, 2015.
776 Massicotte, P., Asmala, E., Stedmon, C., Markager, S.: Global distribution of dissolved matter
777 along the aquatic continuum: Across rivers, lakes and oceans, Sci. Total Environ., 609, 180-
778 191, 2017.
779 McCallister, S. L., and del Giorgio, P. A.: Direct measurement of the $\delta^{13}C$ signature of carbon
780 respired by bacteria in lakes: Linkages to potential carbon sources, ecosystem baseline
781 metabolism, and CO_2 fluxes, Limnol. Oceanogr., 53(4), 1204–1216, 2008.
782 Moody, C. S., Worrall, F., Evans, C. D., Jones, T. G.: The rate of loss of dissolved organic carbon
783 (DOC) through a catchment, J. Hydrol., 492, 139-150, 2013.
784 Moran, M. A., Sheldon, W. M., and Zepp, R. G.: Carbon loss and optical property changes during
785 long-term photochemical and biological degradation of estuarine dissolved organic matter,
786 Limnol. Oceanogr., 45, 1254–1264, 2000.
787 Mostofa, K. M. G., Yoshioka, T., Konohira, E., and Tanoue, E.: Photodegradation of fluorescent
788 dissolved organic matter in river waters, Geochem. J., 41, 323-331, 2007.
789 Mostofa, K. M. G., Wu, F., Liu, C-Q., Vione, D., Yoshioka, T., Sakugawa, H., and Tanoue, E.:
790 Photochemical, microbial and metal complexation behavior of fluorescent dissolved organic
791 matter in the aquatic environments, Geochem. J., 45, 235-254, 2011.
792 Novikov, S. M., Moskvin, Y. P., Trofimov, S. A., Usova, L. I., Batuev, V. I., Tumanovskaya, S. M.,
793 Smirnova, V. P., Markov, M. L., Korotkevicth, A. E., and Potapova, T. M.: Hydrology of bog
794 territories of the permafrost zone of western Siberia, BBM publ. House, St. Petersbourg, 535
795 pp. (in Russian), 2009.
796 Oleinikova, O., Drozdova, O. Y., Lapitskiy, S. A., Bychkov, A. Y., and Pokrovsky, O. S.:
797 Dissolved organic matter degradation by sunlight coagulates organo-mineral colloids and
798 produces low-molecular weight fraction of metals in boreal humic waters, Geochim.
799 Cosmochim. Acta, 211, 97-114, 2017.
800 Oleinikova, O., Shirokova, L. S., Drozdova, O. Y., Lapitsky, S. A., and Pokrovsky, O. S.: Low
801 biodegradability of dissolved organic matter and trace metal from subarctic waters by culturable
802 heterotrophic bacteria, Sci. Total Environ., 618, 174-187, 2018.
803 Page, S. E., Sander, M., Arnold, W. A., and McNeill, K.: Hydroxyl radical formation upon
804 oxidation of reduced humic acids by oxygen in the dark, Environ. Sci. Technol., 46, 1590-
805 1597, 2012.
806 Peacock, M., Evans, C. D., Fenner, N., Freeman, C., Gough, R., Jones, T. G., and Lebron, I.:
807 UV-visible absorbance spectroscopy as a proxy for peatland dissolved organic carbon
808 (DOC) quantity and quality: considerations on wavelength and absorbance degradation,
809 Environmental Science: Processes and Impacts, 10–12, doi:10.1039/c4em00108g, 2014
810 Pickard, A. E., Heal, K. V., McLeod, A. R., and Dinsmore, K. J.: Temporal changes in
811 photoreactivity of dissolved organic carbon and implications for aquatic carbon fluxes from
812 peatlands, Biogeosciences, 14, 1793-1809, https://doi.org/10.5194/bg-14-1793-2017, 2017.

Pokrovsky, O. S., Viers, J., Shirokova, L. S., Shevchenko, V. P., Filipov, A. S., and Dupré, B.: Dissolved, suspended, and colloidal fluxes of organic carbon, major and trace elements in Severnaya Dvina River and its tributary, Chem. Geology, 273, 136–149, 2010.

Pokrovsky, O. S., Shirokova, L. S., Zabelina, S. A., Vorobieva, T. Ya., Moreva, O. Yu., Klimov, S. I., Chupakov, A. V., Shorina, N. V., Kokryatskaya, N. M., Audry, S., Viers, J., Zoutien, C., and Freydier, R.: Size fractionation of trace elements in a seasonally stratified boreal lakes: Control of organic matter and iron colloids, Aquat. Geochem., 18, 115–139, 2012.

Pokrovsky, O. S., Shirokova, L. S., Kirpotin, S. N., Kulizhsky, S. P., Vorobiev, S. N.: Impact of Western Siberia heat wave 2012 on greenhouse gases and trace metal concentration in thaw lakes of discontinuous permafrost zone, Biogeosciences, 10, 5349–5365, 2013.

Pokrovsky, O. S., Manasypov, R. M., Shirokova, L. S., Loiko, S. V., Krickov, I. V., Kopysov, S., and Kirpotin, S. N.: Permafrost coverage, watershed area and season control of dissolved carbon and major elements in western Siberia rivers, Biogeosciences, 12, 6301–6320, 2015.

Pokrovsky, O. S., Manasypov, R. M., Loiko, S. V., and Shirokova, L. S.: Organic and organo-mineral colloids of discontinuous permafrost zone, Geochim. Cosmochim. Acta, 188, 1–20, 2016.

Porcal, P., Dillon, P. J., and Molot, L. A.: Photochemical production and decomposition of particulate organic carbon in a freshwater stream, Aquat. Sci., 75, 469–482, 2013.

Porcal, P., Dillon, P. J., and Molot, L. A.: Interaction of extrinsic chemical factors affecting photodegradation of dissolved organic matter in aquatic ecosystems, Photochem. Photobiol. Sci., 13, 799-812, 2014.

Porcal, P., Dillon, P. J., and Molot, L. A.: Temperature dependence of photodegradation of dissolved organic matter to dissolved inorganic carbon and particulate organic carbon, Plos ONE, 10(6), e0128884, DOI:10.1371/journal.pone.0128884, 2015.

Porter, K. G., and Feig, Y. S.: The use of DAPI for identifying and counting aquatic microflora, Limnol. Oceanogr., 25: 943–948, 1980.

Raudina, T. V., Loiko, S. V., Lim, A., Manasypov, R. M., Shirokova, L. S., Istigecgev, G. I., Kuzmina, D. M., Kulizhsky, S. P., Vorobyev, S. N., and Pokrovsky, O. S.: Permafrost thaw and climate warming may decrease the CO_2, carbon, and metal concentration in peat soil waters of the Western Siberia Lowland, Sci. Total Environ., 634, 1004-1023, 2018.

Reader, H. E., Stedmon, C. A., and Kritzberg, E. S.: Seasonal contribution of terrestrial organic matter and biological oxygen demand to the Baltic Sea from three contrasting river catchments, Biogeosciences 11, 3409-3419, 2014.

Reche, I., Pace, M. L., and Cole, J. J.: Modeled effects of dissolved organic carbon and solar spectra on photobleaching in lake ecosystems, Ecosystems 3, 419-432, 2000.

Roehm, C. L., Giesler, R., Karlsson, J.: Bioavailability of terrestrial organic carbon to lake bacteria: The case of a degrading subarctic permafrost mire complex, J. Geophys. Res., 114, G03006, doi: 10.1029/2008JG000863, 2009.

Selvam, B. P., Lapierre, J.-F., Guillemette, F., Voigt, C., Lamprecht, R. E., Biasi, C., Christensen, T. R., Martikainen P. J., and Berggren, M.: Degradation potentials of dissolved organic carbon (DOC) from thawed permafrost peat. Scientific Reports, 7, Art No 45811, doi: 10.1038/srep45811, 2016.

Serikova, S., Pokrovsky, O. S., Ala-aho, P., Kazantsev, V., Kirpotin, S. N. Kopysov, S. G., Krickov, I. V., Laudon, H., Manasypov, R. M., Shirokova, L. S., Sousby, C., Tetzlaff, D., Karlsson, J.: High riverine CO_2 emissions at the permafrost boundary of Western Siberia. Nature Geoscience, 11, 825-829, 2018.

Serikova S., Pokrovsky O. S., Laudon, H., Krickov, I. V., Lim, A. G., Manasypov, R. M., Karlsson, J.: C emissions from lakes across permafrost gradient of Western Siberia. Nature Comm., 10, Art No 1552, https://doi.org/10.1038/s41467-019-09592-1, 2019.

Shirokova, L. S., Pokrovsky, O. S., Moreva, O. Y., Chupakov, A. V., Zabelina, S. A., Klimov, S. I., Shorina, N. V., and Vorobieva T. Y.: Decrease of concentration and colloidal fraction of organic carbon and trace elements in response to the anomalously hot summer 2010 in a humic boreal lake, Sci. Tot. Environ., 463-464, 78–90, 2013a.

Shirokova, L. S., Pokrovsky, O. S., Kirpotin, S. N., Desmukh, C., Pokrovsky, B. G., Audry, S., and Viers, J.: Biogeochemistry of organic carbon, CO_2, CH_4, and trace elements in thermokarst water bodies in discontinuous permafrost zones of Western Siberia, Biogeochemistry, 113, 573–593, 2013b.

Shirokova, L. S., Bredoire, R., Rolls, J. L., and Pokrovsky, O. S.: Moss and peat leachate degradability by heterotrophic bacteria: fate of organic carbon and trace metals, Geomicrobiol. J., 34(8), 641-655, 2017a.

Shirokova, L. S., Chupakova, A. A., Chupakov, A. V., and Pokrovsky, O.S.: Transformation of dissolved organic matter and related trace elements in the mouth zone of the largest European Arctic river: experimental modeling, Inland Waters, 7(3), 272-282, 2017b.

Spencer, R. G. M., Stubbins, A., Hernes, P. J., Baker, A., Mopper, K., Aufdenkampe, A. K., Dyda, R. Y., Mwamba, V. L., Mangangu, A. M., Wabakanghanzi, J. N., and Six, J.: Photochemical degradation of dissolved organic matter and dissolved lignin phenols from the Congo River, J. Geophys. Res., 114, G03010, doi: 10.1029/2009JG000968, 2009.

Spencer, R. G. M., Mann, P. J., Dittmar, T., Eglinton, T. I., McIntyre, C., Holmes, R. M., Zimov, N., Stubbins, A.: Detecting the signature of permafrost thaw in Arctic rivers, Geophys. Res. Lett., 42, 2830-2835, 2015.

Stubbins, A., Mann, P. J., Powers, L., Bittar, T. B., Dittmar, T., McIntyre, C. P., Eglinton, T. I., Zimov, N., and Spencer, R. G. M.: Low photolability of yedoma permafrost dissolved organic carbon, J. Geophys. Res. Biogeosci., 122, 200-211, doi: 10.1002/2016JG003688, 2017.

Stutter, M. I., Richards, S., and Dawson, J. J. C.: Biodegradability of natural dissolved organic matter collected from a UK moorland stream, Water Res., 47(3), 1169-1180, 2013.

Sulzberger, B., Austin, A. T., Cory, R. M., Zepp, R. G., and Paul, N. D.: Solar UV radiation in a changing world: roles of cryosphere-land-water-atmosphere interfaces in global biogeochemical cycles, Photochem. Photobiol. Sci., doi: 10.1039/c8pp90063a, 2019.

Tarnocai, C., Canadell, J. G., E. Schuur A. G., Kuhry P., Mazhitova G., and Zimov S.: Soil organic carbon pools in the northern circumpolar permafrost region, Global Biogeochem. Cy., 23, GB2023, https://doi.org/10.1029/2008GB003327, 2009.

Textor, S. R., Guillemette, F., Zito, P. A., Spencer, R. G. M.: An assessment of dissolved organic carbon biodegradability and priming in blackwater systems, J. Geophys. Res. Biogeosciences, 123(9), 2998-3015, 2018.

Uyguner, C., and Bekbolet, M. : Implementation of spectroscopic parameters for practical monitoring of natural organic matter, Desalination, 176, 47-55, 2005.

Valle, J., Gonsior, M., Hairir, M., Enrich-Prast, A., Schmitt-Kopplin, P., Bastviken, D., Conrad R., and Hertkorn, N.: Extensive processing of sediment pore water dissolved organic matter during anoxic incubation as observed by high-field mass spectrometry (FTICR-MS), Water Research, 129, 252-263, 2018.

Vähätalo, A. V., Salonen, K., Münster, U., Järvinen, M., and Wetzel, R. G.: Photochemical transformation of allochthonous organic matter provides bioavailable nutrients in a humic lake, Acta Hydrobiol., 156, 287-314, 2003.

Vähätalo, A. V. and Wetzel, R.G.: Photochemical and microbial decomposition of chromophoric dissolved organic matter during long (months-years) exposures, Mar. Chem., 89, 313-326, 2004.

Vasyukova, E., Pokrovsky, O. S., Viers, J., Oliva, P., Dupré, B., Martin, F., and Candaudap, F.: Trace elements in organic- and iron-rich surficial fluids of boreal zone: Assessing colloidal forms via dialysis and ultrafiltration, Geochim. Cosmochim. Acta, 74, 449-468, 2010.

Vonk, J. E., Tank, S. E., Mann, P. J., Spencer, R. G. M., Treat, C. C., Striegl, R. G., Abbott, B. W., and Wickland K. P.: Biodegradability of dissolved organic carbon in permafrost soils and aquatic systems: a meta-analysis, Biogeosciences, 12, 6915-6930, 2015.

Vorobyev, S. N., Pokrovsky O. S., Kolesnichenko, L. G., Manasypov, R. M., Shirokova, L. S., Karlsson, J., and Kirpotin, S. N.: Biogeochemistry of dissolved carbon, major and trace elements during spring flood periods on the Ob River, Hydrol. Processes, 33(11), 1579-1594, 2019.

Ward, C. P., Cory, R. M.: Complete and partial photo-oxidation of dissolved organic matter draining permafrost soils, Environ. Sci. Technol., 50(7), 3545-3553, 2016.

Ward, C. P., Nalven, S. G., Crump, B. C., Kling, G. W., and Cory, R. M.: Photochemical alteration of organic carbon draining permafrost soils shifts microbial metabolic pathways and stimulates respiration, Nature Comm., 8, Art No 772, 2017.

Wauthy M., Rautio, M., Christoffersen, K. S., Forsstrom, L., Laurion, I., Mariash, H. L., Peura, S., Vincent, W. F.: Increasing dominance of terrigenous organic matter in circumpolar freshwaters due to permafrost thaw, Limnol. Oceanogr. Lett., 3, 2018, 186–198, 2012.

Weishaar, J. L., Aiken, G. R., Bergamaschi, B. A., Fram, M. S., Fujii, R., Mopper, K.: Evaluation of specific ultraviolet absorbance as an indicator of the chemical composition and reactivity of dissolved organic carbon, Environ. Sci. Technol., 37, 4702–4708, 2003.

Wickland, K. P., Aiken G. R., Butler K., Dornblaser M. M., Spencer R. G. M., and Striegl R. G.: Biodegradability of dissolved organic carbon in the Yukon River and its tributaries: seasonality and importance of inorganic nitrogen. Glob Biogeochem Cycle 26, 2012gb004342, 2012.

Wilkinson, G. M., Pace, M. L., and Cole, J. J. : Terrestrial dominance of organic matter in north temperate lakes, Global. Biogeochem. Cycles 27, 43-51, 2013.

Winter, A. R., Fish, T. A. E., Playle, R. C., Smith, D. S., and Curtis, P. J.: Photodegradation of natural organic matter from diverse freshwater sources, Aquat. Toxicol., 84, 215-222, 2007.

948

949

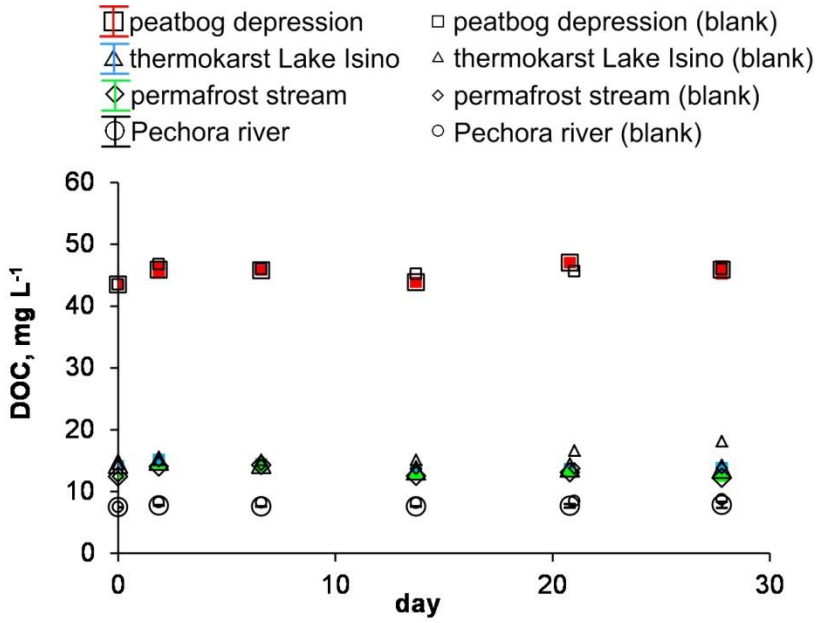

950

951

952 **Fig. 1.** The DOC concentration over time in biodegradation experiments at 23°C. The
953 experiments are shown by solid symbols and the control runs are shown by open symbols: red
954 squares, peatbog depression; green diamonds, permafrost stream; blue triangles, thermokarst
955 Lake Isino, and black circles, the Pechora River. The error bars represent 1 s.d. of three replicates
956 and often within the symbol size.

957

958

959

960

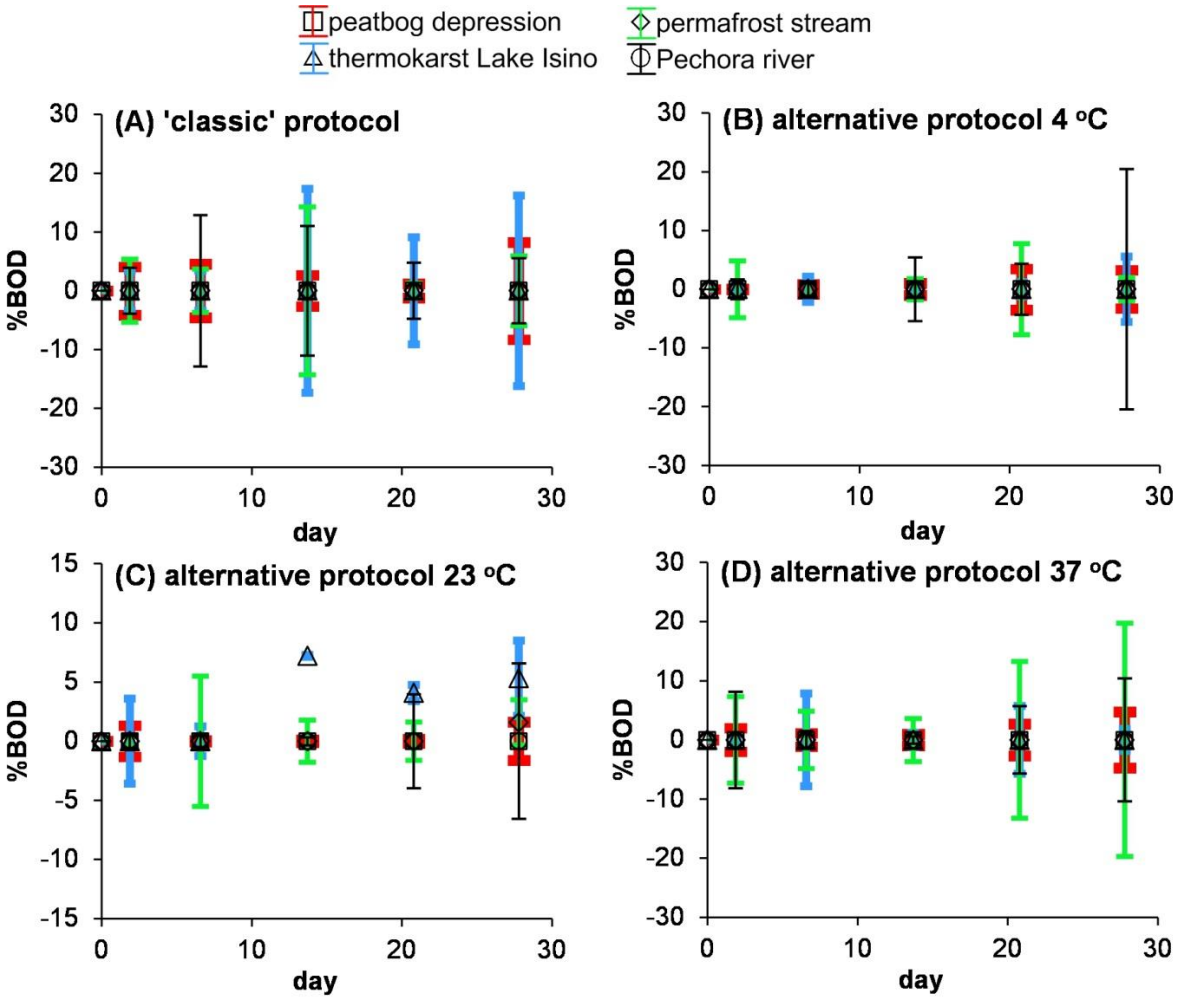

Fig. 2. Percentage of biodegradable DOC as a function of time. **A**, 'classic' protocol (0.7 µm GF/F filtration) at 23°C; **B-D**, alternative protocol of 3 µm - filtered solution incubated at 4°C (B), 23°C (**C**) and 37°C (**D**) and filtered through 0.22 µm at each sampling. The error bars are 1 s.d. of triplicates or, in a few cases, duplicates.

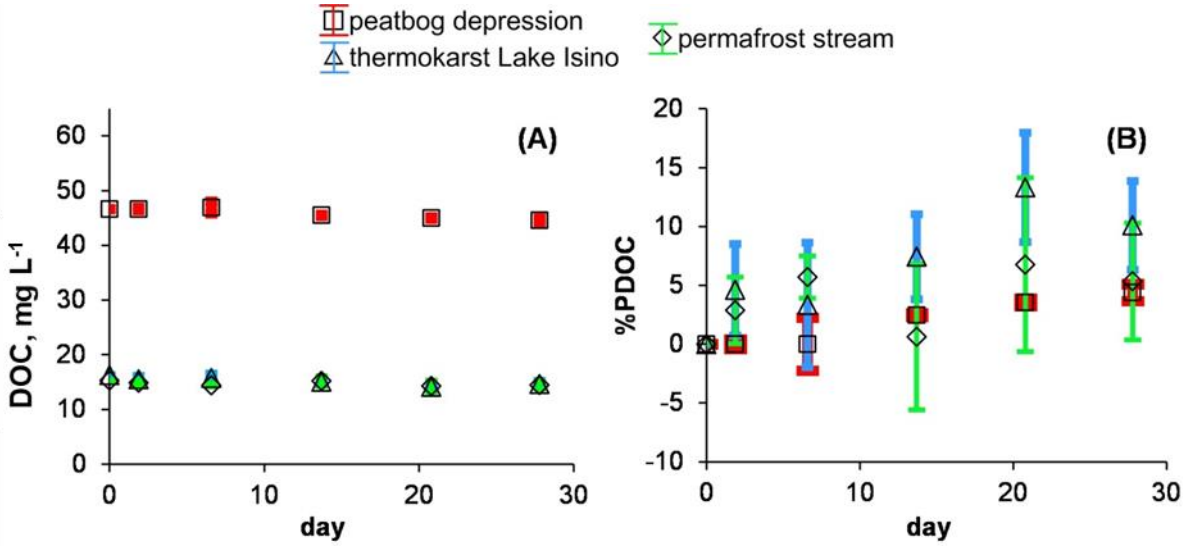

Fig. 3. Concentration (A) and percentage of degradable (B) DOC in photo-degradation experiments. The experiments are shown by solid symbols and the control runs are shown by open symbols: red squares, peatbog depression; green diamonds, permafrost stream; and triangles, thermokarst Lake Isino. The error bars are 1 s.d. of triplicates.

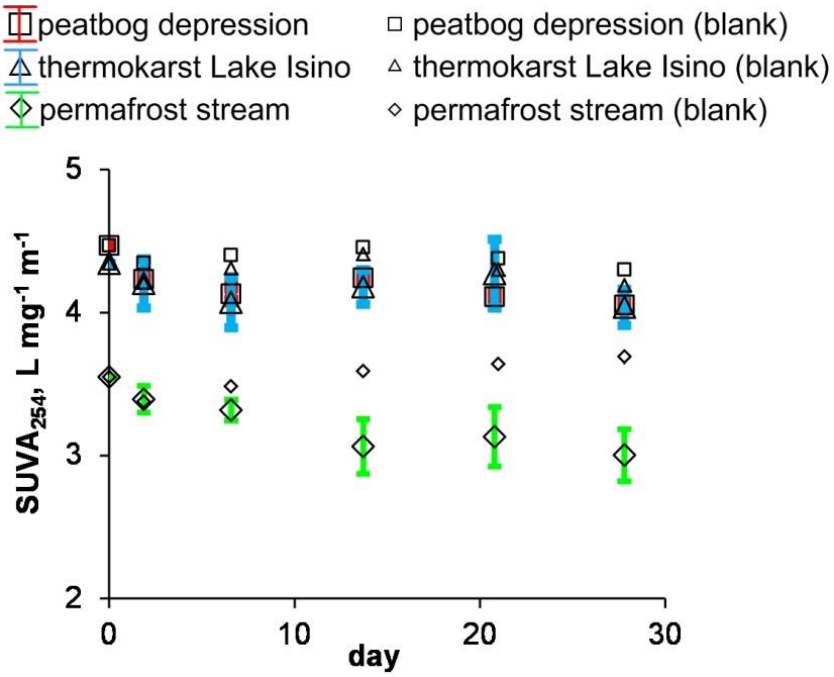

Fig. 4. $SUVA_{254\ nm}$ over time in photo-degradation experiments. The error bars are 1 s.d. of triplicates.

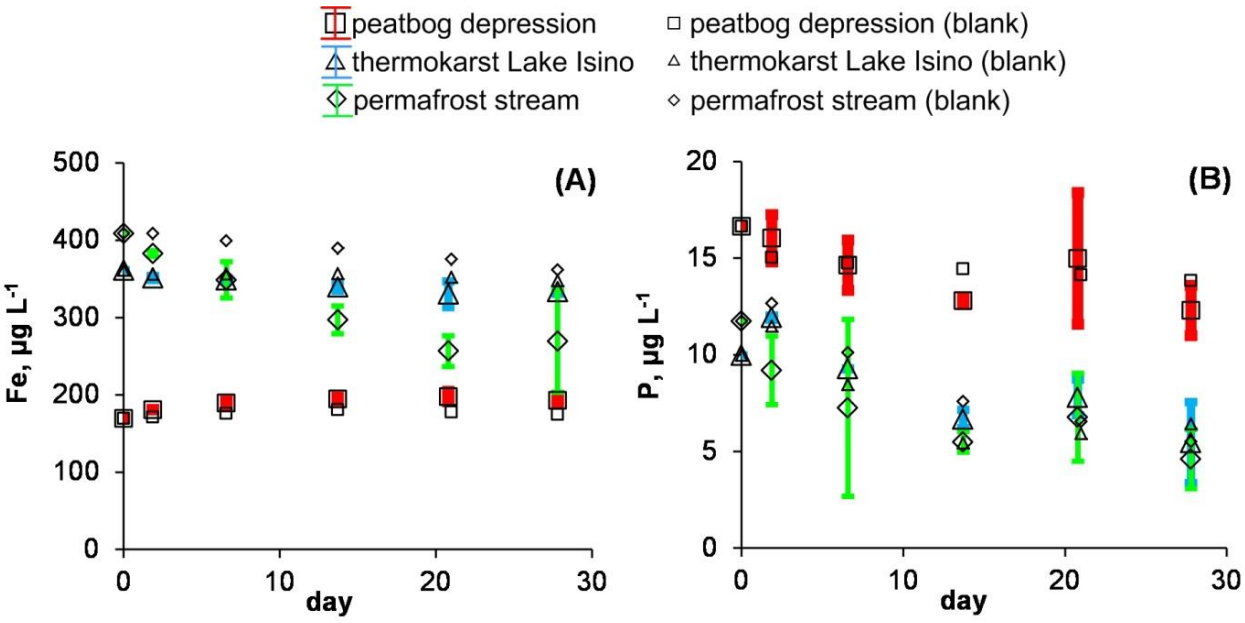

Fig. 5. Fe (A) and P (B) concentration over time in photo-degradation experiments. The error bars are 1 s.d. of triplicates.

Table 1. Landscape setting, hydrochemical characteristics and CO_2 concentration and emission flux of studied waters. S.C. is specific conductivity and TBC is total bacteria count (by DAPI).

Sample	BZ-2-17	BZ-24-17	BZ-12	P5
GPS coordinates	67º36'48,8"N, 53º54'29,8"E	67°36.53'N, 53°50.26'E	67º36'47,7"N, 53º54'38,5"E	$67^0$40'09,4", $52^0$39'30,8"
Description	Depression in peatbog, S_{area} = 7.5 m²	Stream in frozen peatland, $S_{watershed}$ = 7.5 km²	Thermokarst lake (Isino), S_{area} = 0.005 km²	r. Pechora, $S_{watershed}$ = 322,000 km²
T,°C	24	25	24.1	20
pH	3.85	6.52	5.30	6.92
S.C., µS cm^{-1}	59.2	31.5	12.9	65.1
DOC, mg L^{-1}	43.9	16.6	15.6	8.20
DIC, mg L^{-1}	0.992	2.52	0.808	6.11
$SUVA_{254}$	4.08	3.32	4.10	3.82
$P\text{-}PO_4$, µg L^{-1}	2.3	9.8	4.4	26.7
P_{total}, µg L^{-1}	14.6	N.D.	7.3	37.5
$N\text{-}NO_2$, µg L^{-1}	14.6	5.0	3.6	1.67
$N\text{-}NO_3$, µg L-1	14.6	N.D.	76.6	111
$N\text{-}NH_4$, µg L^{-1}	13	152	117	36.5
N_{total}, µg L^{-1}	228	N.D.	200	438
Si, µg L^{-1}	22	392	100	2690
TBC × 10^6, cell mL^{-1}	0.81	5.72	5.36	3.51
pCO_2, ppm	440	2370	1200	1860 (night), 780 (day)
CO_2 flux, mmol m^{-2} d^{-1}	34	30-300*	74	100-130*

Footnote: *, by analogy with small streams of Western Siberian peatlands, of the discontinuous permafrost zone, located in similar environmental context; ** By analogy with Taz and Pur Rivers of western Siberian peatlands (Serikova et al., 2018).